Research Square

Preprints are preliminary reports that have not undergone peer review.
They should not be considered conclusive, used to inform clinical practice,
or referenced by the media as validated information.

Losing sex, keeping gonads: Molecular and ultrastructural signatures of reproductive reorganization in a parthenogenetic earthworm

Irene Sosa

irene.desosa@mncn.csic.es

Museo Nacional de Ciencias Naturales (MNCN-CSIC)

José M. Lorente-Sorolla

Museo Nacional de Ciencias Naturales (MNCN-CSIC)

María Conejero

Museo Nacional de Ciencias Naturales (MNCN-CSIC)

Gemma González-Ponferrada

Museo Nacional de Ciencias Naturales (MNCN-CSIC)

Sergi Taboada

Museo Nacional de Ciencias Naturales (MNCN-CSIC)

Patricia Álvarez-Campos

Universidad Autónoma de Madrid

Ana Riesgo

Museo Nacional de Ciencias Naturales (MNCN-CSIC)

Research Article

Keywords: Parthenogenesis, Earthworms, Hermaphroditism, Gametogenesis, Spermatogenesis, Oogenesis, Gonad transcriptomics, Ultrastructure, Polyploidy, Eiseniella

Posted Date: November 26th, 2026

DOI: https://doi.org/10.21203/rs.3.rs-11772103/v1

License: This work is licensed under a Creative Commons Attribution 4.0 International License.
Read Full License

Additional Declarations: No competing interests reported.

Abstract

Background

The evolution of sexual reproduction remains a central paradox in evolutionary biology, yet nearly 40% of earthworms can reproduce parthenogenetically, offering a model system to explore how reproductive mode shapes gametogenesis at the molecular level. Here, we combined comparative gonad transcriptomics with light and transmission electron microscopy to investigate male and female reproductive pathways in the sexual simultaneous hermaphroditic earthworm *Eiseniella andaluciana* and the closely related parthenogenetic species *Eiseniella tetraedra*.

Results

In *E. andaluciana*, male gonads showed a fully active meiotic and spermatogenic transcriptional program, corroborated by cytophores densely packed with developing germ cells and male funnels filled with mature sperm. In contrast, male gonads of *E. tetraedra* lacked a spermatogenic signature and showed very few male-biased transcripts, with only a tendency towards higher expression of mitochondrial oxidative phosphorylation genes. Histological and ultrastructural observations revealed narrower seminal vesicles with few spermatogenic cells, empty cytophores resembling those of non-reproductive sexual individuals, and no mature sperm, suggesting that spermatogenesis is initiated but rarely completed. Female gonads of *E. tetraedra* displayed the highest transcriptional activity, with upregulation of genes involved in lipid metabolism, maternal mRNA regulation, protein synthesis, oocyte growth and vitellogenesis, indicating a strong investment in yolk provisioning. The comparison of orthologous genes between females of both species showed that meiotic, DNA replication and DNA repair pathways were expressed in both reproductive modes, with higher expression of genes related to DNA replication and chromosome segregation in sexual females and of genes related to the DNA damage response in parthenogenetic females, possibly reflecting the need to maintain genomic stability in a tetraploid genome.

Conclusions

Together, these results suggest that the transition from sexual reproduction to parthenogenesis in earthworms involves a strong reduction of male function and a reorganization, rather than a loss, of female reproductive programs. Our findings provide new molecular and cellular insights into the reproductive changes associated with the loss of sex in hermaphroditic animals.

Background

The evolution of sexual reproduction is one of the most enduring paradoxes in evolutionary biology, as it entails significant initial costs and offers few immediate benefits [1]. Nevertheless, through genetic

recombination, sexual reproduction generates genetic diversity, enabling species to adapt to dynamic and unpredictable environments. Although diverse reproductive strategies exist across metazoans [2], the majority of animal species are gonochoristic, i.e. with separate sexes [3]. In contrast, hermaphrodites can produce both male and female gametes, either simultaneously or sequentially. Hermaphroditism is estimated to occur in 5–6% of animal species, and in nearly one-third of non-insect taxa, with over 70% of animal phyla containing at least one hermaphroditic species [3]. Despite its relatively low overall frequency, hermaphroditism is a widespread reproductive strategy across the tree of life and has evolved multiple times independently throughout animal evolution. Furthermore, it has been proposed as the ancestral sexual condition of animals [2,4]. Besides this variation in female and male functions among species, many animals can also reproduce through parthenogenesis, with the development of embryos from non fertilized eggs, which occurs across nearly all animal phyla [5].

Reproductive strategies in animals are typically shaped by specific ecological and life-history traits [6]. For example, earthworms (Annelida, Crassiclitellata) are generally hermaphroditic invertebrates, and this strategy is believed to be an adaptation to environments where effective population size is low, either due to reduced overall numbers or restricted mobility [6]. By increasing the presence of both functional males and females, reproductive earthworms transform every interaction into a mating opportunity. However, despite being hermaphrodites, 40% of earthworms can reproduce parthenogenetically [7]. Despite being so frequent, parthenogenesis in earthworms has received little attention compared with other groups such as aphids [8], *Daphnia* water fleas [9], *Timema* stick insects [10], bdelloid rotifers [11] or the mud snail *Potamopyrgus antipodarum* [12]. As in hermaphroditism, parthenogenesis has arisen repeatedly during metazoan evolution, most commonly through hybridization between closely related species [13,14]. When two species hybridize, their genomes are often incompatible [15], and this mismatch can disrupt normal meiosis (the cell division that produces sex cells), making sexual reproduction impossible or ineffective, and parthenogenesis can then become the only viable alternative. In earthworms, parthenogenesis has also been linked to hybridization and polyploidy [16–18]. This strategy is particularly advantageous in species with high dispersal capacity and is commonly observed in cosmopolitan earthworms that are readily dispersed through mechanisms such as hydrocory or anthropocory [19,20], since a single individual can establish a new population, conferring them with a high colonization potential.

Regardless of the species being functionally hermaphroditic (sexual) or not (parthenogenetic), most earthworm species have both female and male gonads. The male reproductive system includes the testes, male funnels, seminal vesicles, deferent ducts and male pores, while female system includes the ovaries, ovisacs, female pores and spermatheca which store sperm from the mate [7]. In parthenogenetic species, male structures are functionally unnecessary, and they show variability in number and position [21]. In addition, ultrastructural analyses have shown that oogenesis occurs within germline cysts composed of interconnected cells, called cytophores, where developing oocytes are supported by nurse cells that facilitate cytoplasmic transfer and vitellogenesis [22,23]. Similarly, spermatogenesis takes place in the seminal vesicles, where germ cells develop in synchronous cysts

also organized around a cytophore, supported by somatic cells and cytoskeletal dynamics that regulate germ cell maturation [24,25].

Despite the extensive knowledge on reproductive strategies and morphology in earthworms, the molecular mechanisms underlying the differentiation and function of male and female gonads remain poorly understood. Functionally hermaphroditic earthworms provide a valuable system in which male and female functions coexist within the same individual, potentially leading to trade-offs or conflicts in resource allocation between reproductive roles. In contrast, parthenogenetic lineages do not require fertilization, raising questions about how reproductive pathways are reorganized at the molecular level. In other parthenogenetic animals, the shift to parthenogenesis does not necessarily imply the loss of the genes involved in sexual reproduction, but rather changes in their regulation. For example, the pea aphid *Acyrthosiphon pisum* retains most of the meiotic machinery in a copy number similar to that of other metazoans, but several cell-cycle and meiotic regulatory genes are duplicated, and some of these paralogues are differentially expressed between sexual and parthenogenetic females [8]. In *Daphnia pulex*, obligately parthenogenetic lineages, that arose through hybridization and introgression between two cyclically parthenogenetic species, show altered expression of meiosis and cell-cycle genes, particularly those involved in chromosome segregation, likely as a consequence of regulatory incompatibilities between the parental genomes [26]. Beyond meiosis, parthenogenetic females of *Timema* stick insects show an unexpectedly masculinized pattern of sex-biased gene expression, suggesting that the loss of sex shifts the expression of reproductive genes in females [27]. However, how these pathways are modified in parthenogenetic earthworms has not been explored yet. In particular, it remains unclear whether the male gonads of parthenogenetic earthworms still present an active spermatogenic program or whether this program is reduced. Moreover, it is unknown whether female pathways are conserved across reproductive modes, or whether oogenesis is transcriptionally reprogrammed in the absence of fertilization.

In this context, our study aims to elucidate the molecular mechanisms underlying gametogenesis and the progression from sexual reproduction to parthenogenesis in earthworms. To address this, we use two closely related species, *Eiseniella andaluciana* and *Eiseniella tetraedra* [21], which represent two of the most common reproductive strategies within this group, sexual simultaneous hermaphroditism and parthenogenesis, respectively. By comparing gene expression patterns associated with male and female reproductive pathways, and the ultrastructural features underlying gametogenesis between the functional hermaphroditic and the parthenogenetic species, we aim to assess how reproductive mode influences gametogenic processes that result in parthenogenetic processes.

Methods

Sample collection, tissue dissection and preservation

Specimens were collected in Spain in January 2023. We sampled individuals of *E. andaluciana*, so far known only from its type locality in Salobreña, Granada (36.7337, − 3.5726) [21], and of the cosmopolitan

E. tetraedra in Las Rozas de Madrid (40.5176, − 3.9401) (Additional file 1: Fig. S1). Collected specimens were used for two complementary approaches, comparative transcriptomics of male and female gonads, and light and transmission electron microscopy of the reproductive segments.

For transcriptomic analyses, three specimens per species were dissected prior to tissue preservation. For the male system, testes, sperm funnels and seminal vesicles were extracted from each specimen. For the female system, ovaries, female funnels and ovisacs were extracted individually from *E. andaluciana*, but this was not possible for two of the three specimens of *E. tetraedra* due to their small size; for these two replicates, three female gonads were pooled per sample. In summary, we obtained three biological replicates per reproductive tissue (male and female) for each species (n = 12). Gonadal tissues were fixed in RNAlater Stabilization Solution (Thermo Fisher Scientific Inc.) for 24 h at 4°C and subsequently stored at − 20°C until further processing.

To understand the cytological processes associated with gametogenesis in both reproductive modes, two additional specimens per species were used: one considered reproductive (i.e., undergoing gamete maturation) and one considered non-reproductive (i.e., gamete formation had started but maturation was not occurring). Whole individuals were fixed in 2.5% glutaraldehyde in PBS for 24 h at 4°C. After this initial fixation, samples were rinsed three times in PBS (30 min each) and subsequently stored in 70% ethanol in PBS until further processing.

RNA extraction and cDNA library preparation

We first extracted total RNA from gonads using Invitrogen PureLink RNA Mini Kit with TRIzol™ Reagent (Invitrogen™) following the manufacturer's protocol. RNA concentration was measured with a NanoDrop™ 1000 spectrophotometer (Thermo Fisher Scientific) and RNA quality was determined with the Agilent 4150 TapeStation RNA kit. Then, we purified mRNA and proceeded to cDNA library preparation with an input of 400 ng of mRNA for each sample using the Illumina Stranded mRNA Prep, Ligation Kit (Illumina Inc.) following the manufacturer's recommendations. Resulting libraries had an average insert size of 350 bp. Concentrations of libraries were assessed with Qubit™ 1X dsDNA HS Assay Kit in the Qubit Flex Fluorometer and quality with Agilent 4150 TapeStation D1000 kit. Libraries were multiplexed with Illumina barcodes, and were sequenced in a Novaseq X platform at Novogene (Cambridge, UK) at 150 bp paired-end length.

Sequence processing, de novo assembly and functional annotation

The software FASTQC v. 0.12.1. [28] was used to assess the quality of the raw reads. Adapters and bases with low quality (phred scores < 33) were trimmed off using Trimmomatic v.0.39 [29] using the following parameters: LEADING:25 TRAILING:25 SLIDINGWINDOW:4:15 MINLEN:36. Subsequently, *de novo* transcriptomes (one for species) assemblies were produced using Trinity v.2.13.2 [30], using all the clean reads. Raw sequencing reads have been deposited in the NCBI Sequence Read Archive (SRA) under BioProject accession PRJNA1562945. The completeness of the assembled transcriptome was

evaluated using the gVolante webserver [31], with default settings, employing the BUSCO v.5.1.2 ortholog search pipeline and the metazoan database (metazoa_odb10). The resulting reference transcriptomes were annotated using DIAMOND blastx [32] in more-sensitive mode against the metazoan subset of the UniProtKB/Swiss-Prot database, with an e-value cutoff of 1e − 3. The resulting hits were mapped and annotated in OmicsBox (BioBam) using the Blast2GO suite [33], allowing the assignment of Gene Ontology (GO) terms and the functional characterization of transcripts according to the categories biological process, molecular function, and cellular component.

Differential expression and enrichment analyses

For each species, we obtained gene expression levels comparing males and females, by mapping the reads from each condition to the reference transcriptome of its species using BOWTIE2 v.2.4.4 [34] and estimating transcript abundance with RSEM v.1.2.12 [35] as implemented in Trinity [36]. The package edgeR [37] was used to perform pairwise comparisons between males and females of each species. For *E. andaluciana* the package edgeR was run with the following parameters: false discovery rate (FDR) $p < 0.05$ and min abs (log2(a/b)) change of 1. Visualization of the differentially expressed genes (DGE) between sexes were graphically represented with a hierarchically clustered heatmap generated with the *pheatmap* package [38] in R [39].

For *E. tetraedra*, principal component and sample correlation analyses revealed that one female sample (Ei_3HP) clustered with the male gonad sample from the same individual rather than with the other female replicates (Additional file 2: Fig. S2). This sample was therefore considered an outlier and excluded from the differential expression analysis. Because of the high heterogeneity among the remaining replicates, differential expression was assessed with the quasi-likelihood (QL) framework implemented in edgeR [40]. Lowly expressed transcripts were removed with *filterByExpr*, libraries were normalized with the TMM method, negative binomial (NB) dispersions were estimated with estimateDisp, QL dispersions were estimated with glmQLFit (robust = TRUE), and differential expression between male and female gonads was tested with glmQLFTest. As for *E. andaluciana*, transcripts with FDR < 0.05 and $|\log2FC| \geq 1$ were considered differentially expressed. Given the very low number of male-biased transcripts at this threshold, transcripts with FDR < 0.1 were additionally considered to explore male-biased functional trends. DEGs were represented with a hierarchically clustered heatmap generated with the *pheatmap* package [38] in R [39].

Functional enrichment of the DEGs was assessed with ShinyGO v0.81 [41], using the best BLAST hit gene symbols mapped to the *Homo sapiens* annotation and all protein-coding genes of this species as background. GO biological process terms with FDR < 0.05 were considered significantly enriched.

Light and electron transmission microscopy procedures

For light microscopy, samples were dehydrated through a graded ethanol series (70%, 80%, 96%, and 100%). The final dehydration step in absolute ethanol consisted of three changes of 30 min each. Samples were then cleared in xylene (two changes, 30 min each) and embedded in paraffin at 60°C overnight, with two further paraffin changes to ensure complete embedding. Then, paraffin blocks were mounted with appropriate orientation (transverse and longitudinal sections), and sectioned serially using a microtome Leitz 1512 and dried at 40°C for 24 h. Sections were then stained using a Mallory's trichrome recipe and examined under a light microscope Olympus BX43 with a DP23 camera.

For electron transmission microscopy, post-fixation of samples preserved in glutaraldehyde was performed using 2% osmium tetroxide in PBS for 1 h. Samples were rinsed in PBS (3 × 10 min) and subsequently washed in distilled water (10 min). Dehydration was carried out through an increasing graded ethanol series: 50%, 70%, 80%, 90%, 96%, and 100%, with multiple steps (10 min each) to ensure gradual dehydration. Samples were embedded in LR White resin using a progressive infiltration protocol with ethanol/resin mixtures of increasing resin concentration (1:3, 2:3, 3:1), followed by pure resin infiltration. Each step was performed under rotation for several hours or overnight to ensure proper penetration. Embedded samples were transferred to capsules and polymerized at 60°C for 48 h. Ultrathin sections were obtained with an Ultracut Reichert-Jung ultramicrotome and mounted on copper grids and stained with uranyless for 5 min, followed by lead citrate for 5 min. Observations were performed using JEOL 1010 and JEOL 1400 transmission electron microscopes operated at 80 kV and equipped with Gatan or Megaview II digital imaging systems, at the National Centre for Electron Microscopy (CNME), Complutense University of Madrid, and an APREO 2 field-emission scanning electron microscope (FE-SEM; Thermo Fisher Scientific) operated in scanning transmission electron microscopy (STEM-in-SEM) mode with a bright-field (BF) detector, at the Non-Destructive Techniques Service of the National Museum of Natural Sciences (MNCN-CSIC), Madrid.

Use of AI tools

During the preparation of this work, the authors used Claude (Anthropic) to assist with troubleshooting during data analysis and to improve the language and readability of the manuscript. After using this tool, the authors reviewed and edited the content as needed and take full responsibility for the content of the publication.

Results

De novo assembled transcriptomes of E. andaluciana and E. tetraedra

Sequencing of 12 cDNA libraries generated 321,913 and 403,224 assembled transcripts for *E. andaluciana* and *E. tetraedra*, respectively. The *E. andaluciana* assembly showed higher contiguity (N50 = 1,527 bp) than that of *E. tetraedra* (N50 = 842 bp), although both transcriptomes exhibited similar total assembled lengths (~ 247 versus 249 Mb, respectively). Assessment of transcriptome completeness using BUSCO and the metazoa_odb10 dataset indicated high completeness for both assemblies,

recovering 98.95% and 96.02% complete or fragmented BUSCOs for *E. andaluciana* and *E. tetraedra*, respectively. Detailed sequencing, assembly and transcriptome completeness statistics are provided in Additional file 3: Table S1.

Gene expression patterns and functional enrichment in the sexual species E. andaluciana

Hierarchical clustering analysis grouped our samples by transcriptome-wide similarity in the gonads of *E. andaluciana* differentiating between females and males (Fig. 1A). Main transcriptional differences in the gonads were due to a total of 4,674 differentially expressed genes (DEGs) (Additional file 4: Table S2A). Of these, 4,470 genes were upregulated in male gonads, and 2,311 were functionally annotated (Additional file 4: Table S2A). In contrast, only 204 genes were upregulated in female gonads, with 92 annotated genes (Additional file 4: Table S2A).

In male gonads, several biological processes (BP) related to reproduction were significantly enriched (Fig. 1B, Additional file 4: Table S2B), including GO:0007283 (spermatogenesis), GO:0008584 (male gonad development) and GO:0046661 (male sex differentiation). Additionally, processes related to DNA methylation were also enriched (e.g., GO:0006306 DNA methylation and GO:0043046 DNA methylation involved in gamete generation). At the gene level, several regulators of meiosis and germ cell development were identified upregulated in male gonads, including *DMC1*, *BOLL*, *SYCP3*, *REC8*, *MSH4* and *MLH3*, which are associated with homologous recombination, chromosome synapsis and meiotic progression (Additional file 4: Table S2A).

In female gonads, most enriched biological processes were related to nucleic acid metabolism (Fig. 1C, Additional file 4: Table S2C), including GO:0071897 (DNA biosynthetic process), GO:0006396 (RNA processing), GO:0019859 (thymine metabolic process) and GO:0019860 (uracil metabolic process). Only one GO term not directly related to nucleic acid metabolism was identified (GO:0050688 regulation of defense response to virus). Female-biased expression included genes associated with cellular regulation and maintenance of cellular homeostasis, such as *SODM*, *FGFR4* and *OXR1* (Additional file 4: Table S2A).

Gene expression patterns and functional enrichment in the parthenogenetic species E. tetraedra

Hierarchical clustering analysis also grouped the samples of *E. tetraedra* according to gonad type, differentiating between females and males (Fig. 2A). Main transcriptional differences in the gonads were due to a total of 6,784 differentially expressed genes (DEGs) (Additional file 5: Table S3A). Of these, 6,782 genes were upregulated in female gonads, and 2,160 were functionally annotated (Additional file 5: Table S3A). In contrast, only two genes were upregulated in male gonads, none of which were annotated (Additional file 5: Table S3A).

In male gonads, when a less stringent threshold was applied (FDR < 0.1), several biological processes (BP) related to cellular respiration were significantly enriched (Fig. 2B, Additional file 5: Table S3B), including GO:0006119 (oxidative phosphorylation), GO:0022904 (respiratory electron transport chain) and GO:0015986 (proton motive force-driven ATP synthesis). Additionally, processes related to

proteolysis were also enriched (e.g., GO:0022617 extracellular matrix disassembly and GO:0043171 peptide catabolic process). At the gene level, several mitochondrially encoded subunits of the respiratory chain were identified upregulated in male gonads, including *COX1, COX2, COX3, CYB, ND1, ND2* and *ND3*, together with the ATP synthase subunit *ATP5F1A*, the metalloproteinases *MMP3* and *MMP9* and the aminopeptidases *ENPEP* and *NPEPPS* (Additional file 5: Table S3A).

In female gonads, most enriched biological processes were related to lipid metabolism and protein synthesis (Fig. 2C, Additional file 5: Table S3C), including GO:0006629 (lipid metabolic process), GO:0006664 (glycolipid metabolic process), GO:0006694 (steroid biosynthetic process), GO:0002181 (cytoplasmic translation) and GO:0042254 (ribosome biogenesis). Processes related to intracellular trafficking and degradation (e.g., GO:0007034 vacuolar transport and GO:0010970 transport along microtubule) and to female reproduction (GO:0001541 ovarian follicle development and GO:0008585 female gonad development) were also enriched. Female-biased expression included genes associated with lipid metabolism and storage, such as *FA2H* and *PLIN2*, lysosomal activity, such as *GLB1*, the localization and translational control of maternal mRNAs, such as *STAU1* and *BICD1*, ribosome biogenesis, such as *NOL6*, mitochondrial DNA replication, such as *POLG*, and ubiquitin-mediated protein turnover, such as *NEDD8* and *UBE2O* (Additional file 5: Table S3A).

Comparison between gonads in sexual and parthenogenetic species

A comparison of differentially expressed genes identified in male gonads from *E. andaluciana* and *E. tetraedra* revealed limited overlap between reproductive modes. Only four genes were shared between both reproductive strategies (*BIP*, *HNRPK*, *NUP35* and *QOR*) (Fig. 3A), which are related to processes such as protein folding in the endoplasmic reticulum, RNA processing, nucleocytoplasmic transport and cellular redox balance. Similarly, the comparison of differentially expressed genes identified in female gonads from both species only revealed 22 shared genes between reproductive modes (Fig. 3B), including *ACH1*, *DPYS*, *PTPRM*, *LUCI*, *SBP1B*, *CD109*, *YSM6*, *MYS*, *RFC5*, *OXR1* and *DTX3L*. These genes are mainly associated with general cellular processes like cell–cell recognition in the gonad environment (*PTPRM*), metabolism to meet increasing demands of the oocytes (*ACH1* and *DPYS*), signalling of the TGF-β/BMP pathway (*CD109*), DNA replication (*RFC5*), oxidative stress response (*OXR1*) and cytoskeletal functions (*MYS*). Overall, the low number of shared genes between reproductive modes indicated a limited overlap in sex-biased gene expression.

To further compare females from both reproductive strategies, orthologous transcripts between species were identified as those sharing the same best Swiss-Prot hit, allowing direct comparison of gene expression profiles. We then focused on GO categories related to meiosis, cell cycle, DNA replication and DNA repair, as these processes are central to reproductive cell division and genome maintenance and are expected to play an important role in the molecular mechanisms underlying parthenogenetic reproduction [42,43]. No clear differences were observed in the overall representation of these categories between sexual and parthenogenetic females (Additional file 6: Fig. S3). To investigate these patterns in more detail, we analysed the expression of selected genes associated with these

parthenogenetic processes. Within this subset, we observed differences in the expression of individual genes between reproductive strategies (Fig. 3C). Sexual females showed higher expression of several genes involved in DNA replication, chromosome segregation and cell cycle regulation, including *TOP2A*, *CDC6*, *CENPC*, *CDC27* and *CDN1B*. In contrast, parthenogenetic females exhibited increased expression of genes related to DNA damage response, DNA repair and cytoskeletal dynamics, such as *ATR*, *ZSWM7*, *TBA* and *GCP3*.

Transmission electron and light microscopy of female and male gonads

Transversal sections through the male reproductive region (approximately segment 12) revealed marked differences between the functional hermaphroditic species *E. andaluciana* (Fig. 4A) and the parthenogenetic species *E. tetraedra* (Fig. 4B). In the sexual *E. andaluciana*, the seminal vesicles were larger and densely packed with developing sperm (Fig. 4A). The male funnels also contained abundant mature spermatozoa, which occupied most of the funnel lumen (Fig. 4A). In contrast, *E. tetraedra* showed narrower seminal vesicles, containing fewer developing sperm (Fig. 4B). Moreover, male funnels appeared completely empty of mature spermatozoa, and no sperm masses were observed within the funnel lumen in any of the examined sections (Fig. 4B).

Transmission electron microscopy further highlighted differences in the male reproductive tissues of both species. In the juveniles of *E. andaluciana* cytophores were empty and producing electron-dense bodies that resemble lipid or protein droplets (Fig. 4C), while mature sexual *E. andaluciana*, cytophores were densely packed with developing germ cells (Fig. 4E). Cytophores in both the juvenile and mature *E. tetraedra* were similar to those reported for the juvenile of *E. andaluciana*, also showing electron-dense bodies resembling lipid or protein droplets (Fig. 4D and Fig. 4F, respectively). Moreover, numerous spermatogonia, primary and secondary spermatocytes, and spermatids were observed in the seminal vesicles of *E. andaluciana* radiating from cytophores, indicating ongoing spermatogenesis (Fig. 4E and Additional file 7: Fig. S4), whereas only a few spermatogenic cells were observed in *E. tetraedra*. In the female reproductive region of *E. tetraedra* (approximately in the segment 13th), several cytophore cells containing spermatozoa enclosed within membrane-bound vesicles were observed, with clear signs of cellular degeneration, such as nuclei with a star shape and electron-light appearance (Fig. 4E). These observations are consistent with an active process of sperm engulfment and intracellular digestion within female reproductive tissues.

Discussion

Our comparative transcriptomic analysis revealed marked differences in gonadal gene expression patterns between the sexual earthworm *Eiseniella andaluciana* and the parthenogenetic species *Eiseniella tetraedra*, suggesting that gametogenesis in sexual and parthenogenetic reproductive modes is underpinned by different molecular bases. While the sexual species exhibited transcriptional profiles

consistent with active and functional male and female reproductive pathways, the parthenogenetic lineage showed a reduced transcriptional activity in the male gonads, with a tendency towards higher expression of genes of the mitochondrial oxidative phosphorylation machinery, and an enhanced expression of genes related to lipid metabolism, protein synthesis and intracellular trafficking in the ovaries and oviducts, consistent with an increased investment in oocyte growth and yolk provisioning.

In *E. andaluciana*, the testes and the seminal vesicles showed enrichment of biological processes associated with spermatogenesis, meiosis and male gonad differentiation (Fig. 1B; Additional file 4: Table S2B), indicating a fully functional testis actively engaged in sperm production. We found genes involved in meiotic recombination (e.g., *SPO11*, *RAD51*, *DMC1*, *MSH4* and *MSH5*), chromosome synapsis (e.g., *SYCP3*, *REC8* and *TEX11*) and germ cell differentiation (e.g., *BOLL*, *PIWL1* and *MAEL*) (Additional file 4: Table S2A), all active processes that occur during functional spermatogenesis in animals. In this context, *DMC1* plays a central role in homologous recombination during meiosis, facilitating strand exchange and repair of meiotic double strand breaks [44]. *SYCP3* and *REC8* are essential structural components involved in synaptonemal complex formation and meiotic chromosome cohesion [45]. Similarly, *MSH4* and *MLH3* participate in crossover formation and stabilization of recombination intermediates during meiotic progression [46,47]. In addition, *BOLL* has been widely associated with germ cell differentiation and conserved mechanisms of spermatogenesis in metazoans, including humans and model organisms like *Drosophila melanogaster* and *Caenorhabditis elegans* [48]. The male gonads of *E. andaluciana* also showed a clear enrichment in DNA methylation-related processes. This aligns with the known role of epigenetic regulation in governing germ cell differentiation and chromatin stability during meiosis [49,50]. These findings are consistent with the observed upregulation of *TDRD1*, a Tudor-domain protein critical for piRNA-mediated genome protection [51,52]. Thus, the transcriptional activity in the male gonads confirms that the meiotic machinery is actively driving spermatogenesis in *E. andaluciana*. The histological and ultrastructural findings are consistent with the transcriptomic data. In *E. andaluciana*, we observed abundant developing sperm clustering around the cytophores, a classic feature of earthworm spermatogenesis [24]. This structural integrity, combined with well-preserved sperm morphology, confirms that the species maintains a fully active meiotic program. In contrast, the cytophores of non-reproductive individuals of *E. andaluciana* lacked associated germ cells and contained electron-dense bodies in their cytoplasm, indicating that spermatogenesis had not yet started at this stage.

Male gonads of the parthenogenetic species *E. tetraedra* lacked a clear spermatogenic transcriptional signature. Only two transcripts, neither of them annotated, were significantly upregulated in male gonads, and at a less stringent threshold male-biased transcripts were mainly enriched in processes related to mitochondrial oxidative phosphorylation, including subunits of the respiratory chain such as *COX1*, *COX2*, *COX3*, *CYB*, *ND1*, *ND2* and *ND3*, and the ATP synthase subunit *ATP5F1A* [53]. Although high mitochondrial activity is expected in reproductive tissues due to the energetic demands of gametogenesis, the absence of meiotic and spermatogenic genes suggests that these tissues may no longer sustain fully functional sperm production. In addition, the metalloproteinases *MMP3* and *MMP9*, involved in extracellular matrix degradation and tissue remodelling [54] also tended to be more

expressed in male gonads, which could be related to the structural reorganization of reduced male reproductive tissues. This transcriptomic pattern is congruent with the histological and ultrastructural observations, which revealed narrower seminal vesicles with few developing spermatogenic cells, empty cytophores and male funnels lacking mature sperm. Interestingly, the male reproductive tissues of mature *E. tetraedra* resembled those of juvenile individuals of the sexual *E. andaluciana*, with cytophores containing electron-dense bodies instead of radiating germ cells. Although we cannot rule out that spermatogenesis occurs during a short developmental window that was not captured by our sampling, the scarcity of spermatogenic cells in both juvenile and mature individuals, together with the absence of mature sperm, suggests that spermatogenesis is initiated but rarely completed in this species. This reduction of male function is a common feature in parthenogenetic earthworms. Several parthenogenetic lumbricids have been described as practically male sterile, with spermathecae devoid of sperm [16]. For example, *Aporrectodea trapezoides* retains male reproductive structures such as seminal vesicles and male pores, but shows empty spermathecae and male funnels [55], a pattern very similar to that observed here for *E. tetraedra*. In other oligochaete families, parthenogenetic species show different degrees of degeneration of the male reproductive organs, from reduced spermatogenic activity to the complete loss of testes and seminal vesicles [7,56]. The decay of male traits after the loss of sex has also been reported in other parthenogenetic animals [57], such as the freshwater snail *Potamopyrgus antipodarum*, in which the rare males produced by parthenogenetic lineages show highly variable and frequently abnormal sperm [12]. Jaenike & Selander [58] proposed that, once fertilization is no longer required, selection would favour the reallocation of resources from male to female functions. Under this scenario, the maintenance of fully functional spermatogenesis would be an unnecessary cost for parthenogenetic individuals, which may explain why *E. tetraedra* retains its male gonads but produces few spermatogenic cells and no mature sperm.

Interestingly, female gonads of *E. tetraedra* exhibited the highest transcriptional activity among all analysed tissues. Enriched biological processes among genes upregulated in females relative to male gonads were mainly associated with lipid metabolism (e.g., *ACLY*, *LPIN2*, *DHC24* and *UGCG*), protein synthesis (e.g., *RL3*, *RL5*, *RS6* and *NOL6*), intracellular trafficking (e.g., *VPS41*, *VPS4B* and *KIF3A*) and autophagy (e.g., *ATG4B*, *ATG5* and *GBRL2*). Lipid-related processes were particularly prominent, including glycolipid metabolism, steroid biosynthesis and protein localization to lipid droplets, and several upregulated genes, such as *FA2H* and *PLIN2*, are involved in membrane lipid remodelling and intracellular lipid storage, respectively [59,60]. Lipid accumulation is a key component of oogenesis, particularly during yolk formation and embryonic provisioning. In parthenogenetic species, this metabolic investment may be especially relevant as the energy saved by skipping the cost of sex is often reallocated toward enhanced maternal provisioning to ensure autonomous embryonic success [19,61]. Such a strategy would be particularly advantageous for parthenogenetic earthworms, which are often cosmopolitan in distribution [62,63]. Thus, the strong expression of lipid-related genes in female gonads of *E. tetraedra* likely reflects a specialized reproductive–colonization strategy: by maximizing offspring fitness through high-quality yolk, parthenogenesis enables a single individual to not only establish a new

population but to do so with highly competitive potential, conferring the exceptional colonization success observed in parthenogenetic species.

In addition to lipid metabolism, the female gonads of *E. tetraedra* showed a much larger number of upregulated genes in females relative to male gonads (1,783 annotated genes) than those of *E. andaluciana* (69), many of them associated with oocyte growth. Consistently, GO terms directly related to female reproduction, such as ovarian follicle development and female gonad development, were also enriched. In the female gonads of *E. tetraedra*, genes involved in the localization and translational control of maternal mRNAs, such as *STAU1* and *BICD1*, were upregulated relative to male gonads. *BICD1* is required for oocyte differentiation in *Drosophila melanogaster* [64], and *STAU1* encodes Staufen, a key component of the machinery that localizes maternal mRNAs during oogenesis [65]. Similarly, processes related to protein synthesis, such as ribosome biogenesis and cytoplasmic translation, were enriched, together with genes such as *NOL6* and the mitochondrial DNA polymerase *POLG*, consistent with the accumulation of ribosomes and the amplification of mtDNA that characterize growing oocytes [66]. Female gonads of *E. tetraedra* also showed higher expression than male gonads of genes linked to ubiquitin-mediated turnover (*NEDD8* and *UBE2O*) [67,68], lysosomal hydrolases (*GLB1*, *CATC* and *CATZ*) [69,70], and endocytosis and actin remodelling (*LRP1*, *MPRD* and *FLNA*) [71]. Rather than reflecting a degradative process, this signature is consistent with active vitellogenesis. In oviparous animals, yolk precursors are incorporated into the oocyte through receptor-mediated endocytosis by members of the low-density lipoprotein receptor family, to which *LRP1* belongs [72,73], and are subsequently processed within the oocyte by lysosomal cathepsins [74]. Together, these results indicate that oogenesis is not only conserved in *E. tetraedra* but may be intensified, with an enhanced investment in oocyte growth and yolk provisioning. However, as these comparisons were performed against male gonads, the larger number of female-biased genes in *E. tetraedra* may also partly reflect the reduced activity of its male gonads.

Despite the major differences observed between reproductive modes, the direct comparison of female gonads between species showed that several pathways associated with meiosis, DNA replication and DNA repair remained partially conserved. This result suggests that parthenogenesis in *E. tetraedra* does not involve a complete suppression of canonical reproductive pathways, but rather a partial rewiring of them. Indeed, while sexual *E. andaluciana* females showed higher expression of genes related to DNA replication, chromosome segregation and cell cycle progression, such as *TOP2A*, *CDC6* and *CENPC*, parthenogenetic *E. tetraedra* females preferentially expressed genes associated with DNA repair and cellular regulation, including *ATR* and *ZSWM7*. These results are particularly significant given the tetraploid nature of *E. tetraedra* [75]. Managing four sets of chromosomes during meiotic parthenogenesis may impose substantial challenges to genomic integrity due to the increased risk of aberrant chromosomal pairing and segregation in polyploid meiosis [76]. In this context, the higher expression of *ATR*, the central kinase of the DNA damage checkpoint, and *ZSWM7*, which has been associated with meiotic recombination and chromosome dynamics, suggests enhanced investment in genome surveillance and chromosomal maintenance mechanisms [77,78]. Such transcriptional shifts may contribute to preserving genomic stability in these polyploid parthenogenetic lineages and could

help mitigate the accumulation of deleterious mutations typically predicted under Muller's ratchet in asexual populations [79].

Conclusions

Our results reveal clear differences in gonadal function between the sexual *E. andaluciana* and the parthenogenetic *E. tetraedra*. In *E. tetraedra*, male gonads are retained but spermatogenesis appears to be initiated and rarely completed, as shown by the lack of a spermatogenic transcriptional signature, the scarcity of spermatogenic cells and the absence of mature sperm. In contrast, oogenesis is conserved and may even be enhanced, with a strong signature of lipid metabolism, oocyte growth and yolk provisioning. Overall, our results suggest that the transition to parthenogenesis in earthworms involves a strong reduction of male function and a reorganization, rather than a loss, of female reproductive programs. By integrating gonad transcriptomics with light and electron microscopy, this study provides the first comparative characterization of male and female gonads between a sexual and a parthenogenetic earthworm. As it focuses on a single pair of closely related species, extending this approach to additional sexual and parthenogenetic lineages, ideally representing independent origins of parthenogenesis, and to different stages of the reproductive cycle will help determine how general these patterns are. Future work combining genomic resources and cytological analyses of oocyte meiosis will further clarify how parthenogenetic earthworms regulate gametogenesis and maintain genome stability in the absence of fertilization.

Abbreviations

BP
biological process
BUSCO
Benchmarking Universal Single-Copy Orthologs
DEG
differentially expressed gene
FDR
false discovery rate
GO
Gene Ontology
log2FC
log2 fold change
NB
negative binomial
QL
quasi-likelihood
STEM
scanning transmission electron microscopy

TEM
transmission electron microscopy
TMM
trimmed mean of M-values.

Declarations

Declarations

Ethics approval and consent to participate

Not applicable. This study used earthworms (Annelida), which are not subject to animal experimentation regulations.

Consent for publication

Not applicable.

Competing interests

The authors declare that they have no competing interests.

Additional files

Additional file 1: Fig. S1.

(.pdf) Sampling localities of *E. andaluciana* (Salobreña, Granada) and *E. tetraedra* (Las Rozas de Madrid) in Spain.

Additional file 2: Fig. S2.

(.pdf) Principal component analysis and sample correlation of the six *E. tetraedra* gonad libraries, showing that the female sample Ei_3HP clusters with the male gonad sample from the same individual.

Additional file 3: Table S1.

(.xlsx) Sequencing, *de novo* assembly and transcriptome completeness (BUSCO, metazoa_odb10) statistics for *E. andaluciana* and *E. tetraedra*.

Additional file 4: Table S2.

(.xlsx) Differential expression and functional enrichment in gonads of *E. andaluciana*. A: Differentially expressed transcripts between male and female gonads (FDR < 0.05, |log2FC| ≥ 1) with functional

annotation. B: GO biological process terms enriched among male-upregulated genes. C: GO biological process terms enriched among female-upregulated genes.

Additional file 5: Table S3.

(.xlsx) Differential expression and functional enrichment in gonads of *E. tetraedra* (edgeR quasi-likelihood, Ei_3HP excluded). A: Differentially expressed transcripts between male and female gonads with functional annotation (female-upregulated, FDR < 0.05, |log2FC| ≥ 1; male-upregulated, FDR < 0.1). B: GO biological process terms enriched among male-upregulated genes (FDR < 0.1). C: GO biological process terms enriched among female-upregulated genes.

Additional file 6: Fig. S3.

(.pdf) Expression of orthologous genes associated with meiosis, cell cycle, DNA replication and DNA repair in female gonads of the sexual *E. andaluciana* and the parthenogenetic *E. tetraedra*. Heatmap of mean expression (log10(TMM + 1)) for orthologous genes (same best Swiss-Prot hit) annotated with these GO categories.

Additional file 7: Fig. S4.

(.pdf) Transmission electron micrograph of the seminal vesicles of a reproductive specimen of *E. andaluciana*, showing spermatogonia, primary and secondary spermatocytes and spermatids radiating from a cytophore. Scale bar: 10 µm.

Funding

I.d.S. was funded by the European Union-Next GenerationEU program through a Margarita Salas fellowship and JdC (Juan de la Cierva, 2024) personal grant (JDC2024-054954-I). J.M.L-S. was supported by a predoctoral fellowship (PRE2020-095330) funded by MCIN/AEI/10.13039/501100011033. S.T. received funding from the grant PID2024-159957NB-I00 funded by MCIN/AEI/10.13039/501100011033 and from the grant CNS2023-144572 and by the Ramón y Cajal grant RYC2021-03152-I, funded by the MCIN/AEI/10.13039/501100011033 and the European Union «NextGenerationEU»/PRTR». P.Á-C received funding from the Spanish Government AEI/10.13039/501100011033 (grant PID2023-148497NA-I00) and from the European Union “Next Generation EU”/PRTR (grant CNS2023-145193). A.R. received funding from the grant PID2019-105769GB-I00, funded by the Spanish agencies MCIN/AEI/10.13039/50110001103 and EI “FSE invierte en tu futuro” and acknowledges funding from the European grant “Biodiversity Genomics Europe” (Grant agreement ID: 101059492).

Author Contribution

I.d.S., P.Á.-C. and A.R. conceived and designed the study. I.d.S. and P.Á.-C. collected the samples. I.d.S. and J.M.L.-S. performed the laboratory work. I.d.S., G.G.-P., M.C. and A.R. performed the microscopy. I.d.S. and S.T. analysed the data. I.d.S. wrote the first draft of the manuscript. All authors read, revised and approved the final manuscript.

Acknowledgement

We are grateful to Daniel Ruíz Buck for his hospitality during fieldwork in Salobreña (Granada).

Data Availability

The datasets generated and analysed during the current study are available in the NCBI Sequence Read Archive repository, BioProject PRJNA1562945 (https://www.ncbi.nlm.nih.gov/bioproject/PRJNA1562945). Differential expression and functional enrichment results are included within the article and its additional files (Additional files 4 and 5). The scripts used for the bioinformatic analyses are available in the Zenodo repository (https://doi.org/10.5281/zenodo.24291118).

References

1. 1. Subramoniam T. Mode of reproduction: invertebrate animals. In: Skinner MK, editor. Encyclopedia of reproduction. 2nd ed., vol. 6. Oxford: Academic Press; 2018. p. 32–40.
2. 2. Sasson DA, Ryan JF. A reconstruction of sexual modes throughout animal evolution. BMC Evol Biol. 2017;17:242.
3. 3. Jarne P, Auld JR. Animals mix it up too: the distribution of self-fertilization among hermaphroditic animals. Evolution. 2006;60:1816–24.
4. 4. Riesgo A, Novo M, Sharma PP, Peterson M, Maldonado M, Giribet G. Inferring the ancestral sexuality and reproductive condition in sponges (Porifera). Zool Scr. 2014;43:101–17.
5. 5. Sperling AL, Glover DM. Parthenogenesis in dipterans: a genetic perspective. Proc Biol Sci. 2023;290:20230261.
6. 6. Clark WC. Hermaphroditism as a reproductive strategy for metazoans; some correlated benefits. N Z J Zool. 1978;5:769–80.
7. 7. Díaz Cosín DJ, Novo M, Fernández R. Reproduction of earthworms: sexual selection and parthenogenesis. In: Karaca A, editor. Biology of earthworms. Soil Biology, vol. 24. Berlin: Springer; 2011. p. 69–86.
8. 8. Srinivasan DG, Fenton B, Jaubert-Possamai S, Jaouannet M. Analysis of meiosis and cell cycle genes of the facultatively asexual pea aphid, *Acyrthosiphon pisum* (Hemiptera: Aphididae). Insect Mol Biol. 2010;19 Suppl 2:229–39.

9. 9. Tucker AE, Ackerman MS, Eads BD, Xu S, Lynch M. Population-genomic insights into the evolutionary origin and fate of obligately asexual *Daphnia pulex*. Proc Natl Acad Sci U S A. 2013;110:15740–5.
10. 10. Schwander T, Henry L, Crespi BJ. Molecular evidence for ancient asexuality in *Timema* stick insects. Curr Biol. 2011;21:1129–34.
11. 11. Flot JF, Hespeels B, Li X, Noel B, Arkhipova I, Danchin EGJ, et al. Genomic evidence for ameiotic evolution in the bdelloid rotifer *Adineta vaga*. Nature. 2013;500:453–7.
12. 12. Jalinsky J, Logsdon JM Jr, Neiman M. Male phenotypes in a female framework: evidence for degeneration in sperm produced by male snails from asexual lineages. J Evol Biol. 2020;33:1050–9.
13. 13. Avise JC, Quattro JM, Vrijenhoek RC. Molecular clones within organismal clones: mitochondrial DNA phylogenies and the evolutionary histories of unisexual vertebrates. Evol Biol. 1992;26:225–46.
14. 14. Mantovani B. Satellite sequence turnover in parthenogenetic systems: the apomictic triploid hybrid *Bacillus lynceorum* (Insecta, Phasmatodea). Mol Biol Evol. 1998;15:1288–97.
15. 15. Fyon F, Berbel-Filho WM, Schlupp I, Wild G, Úbeda F. Why do hybrids turn down sex? Evolution. 2023;77:2186–99.
16. 16. Muldal S. The chromosomes of the earthworms. I. The evolution of polyploidy. Heredity. 1952;6:55–76.
17. 17. Viktorov AG. Diversity of polyploid races in the family Lumbricidae. Soil Biol Biochem. 1997;29:217–21.
18. 18. de Sosa I, Turon M, Taboada S, Lorente-Sorolla JM, Fernández R, Tilikj N, et al. No mate, no problem: molecular mechanisms involved in parthenogenesis in the cosmopolitan earthworm *Aporrectodea trapezoides* (Annelida, Clitellata). Mol Ecol. 2025;34:e70010.
19. 19. Terhivuo J, Saura A. Dispersal and clonal diversity of North-European parthenogenetic earthworms. Eur J Soil Biol. 2006;42 Suppl 1:S201–5.
20. 20. de Sosa I, Fernández Marchán D, Novo M, Díaz Cosín DJ, Giribet G, Fernández R. Insights into the origin of parthenogenesis in oligochaetes: strong genetic structure in a cosmopolitan earthworm is not related to reproductive mode. Eur J Soil Biol. 2017;81:31–8.
21. 21. de Sosa I, Marchán DF, Novo M, Szederjesi T, Jelić M, Jabłońska A, et al. Guess who? Taxonomic problems in the genus *Eiseniella* revisited by integrated approach. Org Divers Evol. 2023;23:295–308.
22. 22. Świątek P, Kubrakiewicz J, Klag J. Formation of germ-line cysts with a central cytoplasmic core is accompanied by specific orientation of mitotic spindles and partitioning of existing intercellular bridges. Cell Tissue Res. 2009;337:137–48.
23. 23. Świątek P, Urbisz AZ. Architecture and life history of female germ-line cysts in clitellate annelids. In: Kloc M, Kubiak JZ, editors. Evo-Devo: non-model species in cell and developmental biology. Results and Problems in Cell Differentiation, vol. 68. Cham: Springer; 2019. p. 515–51.
24. 24. Jamieson BGM. The ultrastructure of the Oligochaeta. London: Academic Press; 1981.

25. 25. Małota K, Świątek P. Analysis of the cytoskeleton organization and its possible functions in male earthworm germ-line cysts equipped with a cytophore. Cell Tissue Res. 2016;366:175–89.
26. 26. Snyman M, Xu S. Transcriptomics and the origin of obligate parthenogenesis. Heredity. 2023;131:119–29.
27. 27. Parker DJ, Bast J, Jalvingh K, Dumas Z, Robinson-Rechavi M, Schwander T. Sex-biased gene expression is repeatedly masculinized in asexual females. Nat Commun. 2019;10:4638.
28. 28. Andrews S. FastQC: a quality control tool for high throughput sequence data. 2010. https://www.bioinformatics.babraham.ac.uk/projects/fastqc/.
29. 29. Bolger AM, Lohse M, Usadel B. Trimmomatic: a flexible trimmer for Illumina sequence data. Bioinformatics. 2014;30:2114–20.
30. 30. Haas BJ, Papanicolaou A, Yassour M, Grabherr M, Blood PD, Bowden J, et al. De novo transcript sequence reconstruction from RNA-seq using the Trinity platform for reference generation and analysis. Nat Protoc. 2013;8:1494–512.
31. 31. Nishimura O, Hara Y, Kuraku S. gVolante for standardizing completeness assessment of genome and transcriptome assemblies. Bioinformatics. 2017;33:3635–7.
32. 32. Buchfink B, Xie C, Huson DH. Fast and sensitive protein alignment using DIAMOND. Nat Methods. 2015;12:59–60.
33. 33. Götz S, García-Gómez JM, Terol J, Williams TD, Nagaraj SH, Nueda MJ, et al. High-throughput functional annotation and data mining with the Blast2GO suite. Nucleic Acids Res. 2008;36:3420–35.
34. 34. Langmead B, Salzberg SL. Fast gapped-read alignment with Bowtie 2. Nat Methods. 2012;9:357–9.
35. 35. Li B, Dewey CN. RSEM: accurate transcript quantification from RNA-Seq data with or without a reference genome. BMC Bioinformatics. 2011;12:323.
36. 36. Grabherr MG, Haas BJ, Yassour M, Levin JZ, Thompson DA, Amit I, et al. Full-length transcriptome assembly from RNA-Seq data without a reference genome. Nat Biotechnol. 2011;29:644–52.
37. 37. Robinson MD, McCarthy DJ, Smyth GK. edgeR: a Bioconductor package for differential expression analysis of digital gene expression data. Bioinformatics. 2010;26:139–40.
38. 38. Kolde R. pheatmap: pretty heatmaps. R package version 1.0.12. 2019. https://CRAN.R-project.org/package=pheatmap.
39. 39. R Core Team. R: a language and environment for statistical computing. Vienna: R Foundation for Statistical Computing; 2024. https://www.R-project.org/.
40. 40. Chen Y, Lun ATL, Smyth GK. From reads to genes to pathways: differential expression analysis of RNA-Seq experiments using Rsubread and the edgeR quasi-likelihood pipeline. F1000Res. 2016;5:1438.

41. 41. Ge SX, Jung D, Yao R. ShinyGO: a graphical gene-set enrichment tool for animals and plants. Bioinformatics. 2020;36:2628–9.
42. 42. Schurko AM, Logsdon JM Jr, Eads BD. Meiosis genes in *Daphnia pulex* and the role of parthenogenesis in genome evolution. BMC Evol Biol. 2009;9:78.
43. 43. Neiman M, Sharbel TF, Schwander T. Genetic causes of transitions from sexual reproduction to asexuality in plants and animals. J Evol Biol. 2014;27:1346–59.
44. 44. Cloud V, Chan YL, Grubb J, Budke B, Bishop DK. Rad51 is an accessory factor for Dmc1-mediated joint molecule formation during meiosis. Science. 2012;337:1222–5.
45. 45. Yuan L, Liu JG, Zhao J, Brundell E, Daneholt B, Höög C. The murine SCP3 gene is required for synaptonemal complex assembly, chromosome synapsis, and male fertility. Mol Cell. 2000;5:73–83.
46. 46. Nishant KT, Rao MRS. Molecular features of meiotic recombination hot spots. Bioessays. 2006;28:45–56.
47. 47. Roesner LM, Mielke C, Faehnrich S, Merkhoffer Y, Dittmar KE, Drexler HG, et al. Localization of MLH3 at the centrosomes. Int J Mol Sci. 2014;15:13932–7.
48. 48. Xu EY, Moore FL, Reijo Pera RA. A gene family required for human germ cell development evolved from an ancient meiotic gene conserved in metazoans. Proc Natl Acad Sci U S A. 2001;98:7414–9.
49. 49. Hackett JA, Surani MA. DNA methylation dynamics during the mammalian life cycle. Philos Trans R Soc Lond B Biol Sci. 2013;368:20110328.
50. 50. Jenkins TG, Carrell DT. The sperm epigenome and potential implications for the developing embryo. Reproduction. 2012;143:727–34.
51. 51. Chuma S, Hosokawa M, Kitamura K, Kasai S, Fujioka M, Hiyoshi M, et al. Tdrd1/Mtr-1, a tudor-related gene, is essential for male germ-cell differentiation and nuage/germinal granule formation in mice. Proc Natl Acad Sci U S A. 2006;103:15894–9.
52. 52. Yabuta Y, Ohta H, Abe T, Kurimoto K, Chuma S, Saitou M. TDRD5 is required for retrotransposon silencing, chromatoid body assembly, and spermiogenesis in mice. J Cell Biol. 2011;192:781–95.
53. 53. Castellana S, Vicario S, Saccone C. Evolutionary patterns of the mitochondrial genome in Metazoa: exploring the role of mutation and selection in mitochondrial protein-coding genes. Genome Biol Evol. 2011;3:1067–79.
54. 54. Page-McCaw A, Ewald AJ, Werb Z. Matrix metalloproteinases and the regulation of tissue remodelling. Nat Rev Mol Cell Biol. 2007;8:221–33.
55. 55. Fernández R, Novo M, Gutiérrez M, Almodóvar A, Díaz Cosín DJ. Life cycle and reproductive traits of the earthworm *Aporrectodea trapezoides* (Dugès, 1828) in laboratory cultures. Pedobiologia. 2010;53:295–9.
56. 56. Shen HP, Tsai CF, Fang YP, Chen JH. Parthenogenesis, polyploidy and reproductive seasonality in the Taiwanese mountain earthworm *Amynthas catenus* Tsai et al., 2001 (Oligochaeta, Megascolecidae). Pedobiologia. 2011;54:133–9.

57. 57. van der Kooi CJ, Schwander T. On the fate of sexual traits under asexuality. Biol Rev Camb Philos Soc. 2014;89:805–19.
58. 58. Jaenike J, Selander RK. Evolution and ecology of parthenogenesis in earthworms. Am Zool. 1979;19:729–37.
59. 59. Eckhardt M. Fatty acid 2-hydroxylase and 2-hydroxylated sphingolipids: metabolism and function in health and diseases. Int J Mol Sci. 2023;24:4908.
60. 60. Ajjaji D, Ben M'barek K, Mimmack ML, England C, Herscovitz H, Dong L, et al. Dual binding motifs underpin the hierarchical association of perilipins1–3 with lipid droplets. Mol Biol Cell. 2019;30:703–16.
61. 61. Judson OP, Normark BB. Ancient asexual scandals. Trends Ecol Evol. 1996;11:41–6.
62. 62. Gates GE. Burmese earthworms: an introduction to the systematics and biology of megadrile oligochaetes with special reference to Southeast Asia. Trans Am Philos Soc. 1972;62:1–326.
63. 63. Sims RW, Gerard BM. Earthworms: notes for the identification of British species. 4th ed. Synopses of the British Fauna (New Series), No. 31. Shrewsbury: Field Studies Council; 1999.
64. 64. Suter B, Steward R. Requirement for phosphorylation and localization of the Bicaudal-D protein in *Drosophila* oocyte differentiation. Cell. 1991;67:917–26.
65. 65. St Johnston D, Beuchle D, Nüsslein-Volhard C. *staufen*, a gene required to localize maternal RNAs in the *Drosophila* egg. Cell. 1991;66:51–63.
66. 66. Spikings EC, Alderson J, St John JC. Regulated mitochondrial DNA replication during oocyte maturation is essential for successful porcine embryonic development. Biol Reprod. 2007;76:327–35.
67. 67. Komander D, Rape M. The ubiquitin code. Annu Rev Biochem. 2012;81:203–29.
68. 68. Huang DT, Miller DW, Mathew R, Cassell R, Holton JM, Roussel MF, et al. A unique E1–E2 interaction required for optimal conjugation of the ubiquitin-like protein NEDD8. Nat Struct Mol Biol. 2004;11:927–35.
69. 69. Turk V, Stoka V, Vasiljeva O, Renko M, Sun T, Turk B, et al. Cysteine cathepsins: from structure, function and regulation to new frontiers. Biochim Biophys Acta. 2012;1824:68–88.
70. 70. Bonten EJ, Annunziata I, d'Azzo A. Lysosomal multienzyme complex: pros and cons of working together. Cell Mol Life Sci. 2014;71:2017–32.
71. 71. McMahon HT, Boucrot E. Molecular mechanism and physiological functions of clathrin-mediated endocytosis. Nat Rev Mol Cell Biol. 2011;12:517–33.
72. 72. Schneider WJ. Vitellogenin receptors: oocyte-specific members of the low-density lipoprotein receptor supergene family. Int Rev Cytol. 1996;166:103–37.
73. 73. Spinsante C, Carducci F, Carotti E, Canapa A, Bizzaro D, Biscotti MA, et al. A bioinformatic approach to characterize the vitellogenin receptor and the low density lipoprotein receptor superfamily in the newt *Cynops orientalis*. Sci Rep. 2025;15. doi:10.1038/s41598-025-88011-6.

74. 74. Carnevali O, Cionna C, Tosti L, Lubzens E, Maradonna F. Role of cathepsins in ovarian follicle growth and maturation. Gen Comp Endocrinol. 2006;146:195–203.
75. 75. Casellato S. On polyploidy in oligochaetes with particular reference to lumbricids. In: Bonvicini Pagliai AM, Omodeo P, editors. On earthworms. Selected Symposia and Monographs U.Z.I., 2. Modena: Mucchi; 1987. p. 75–87.
76. 76. Comai L. The advantages and disadvantages of being polyploid. Nat Rev Genet. 2005;6:836–46.
77. 77. Delacroix S, Wagner JM, Kobayashi M, Yamamoto K, Karnitz LM. The Rad9–Hus1–Rad1 (9-1-1) clamp activates checkpoint signaling via TopBP1. Genes Dev. 2007;21:1472–7.
78. 78. McGlacken-Byrne SM, Le Quesne Stabej P, Del Valle I, Ocaka L, Gagunashvili A, Crespo B, et al. ZSWIM7 is associated with human female meiosis and familial primary ovarian insufficiency. J Clin Endocrinol Metab. 2022;107:e254–63.
79. 79. Schurko AM, Neiman M, Logsdon JM Jr. Signs of sex: what we know and how we know it. Trends Ecol Evol. 2009;24:208–17.
80. 80. NCBI Sequence Read Archive. BioProject PRJNA1562945: gonad transcriptomes of *Eiseniella andaluciana* and *Eiseniella tetraedra*. https://www.ncbi.nlm.nih.gov/bioproject/PRJNA1562945.
81. 81. de Sosa I, Lorente-Sorolla JM, Conejero M, González-Ponferrada G, Taboada S, Álvarez-Campos P, Riesgo A. Scripts for: Losing sex, keeping gonads: molecular and ultrastructural signatures of reproductive reorganization in a parthenogenetic earthworm. Zenodo. 2026. https://doi.org/10.5281/zenodo.24291118.

Figures

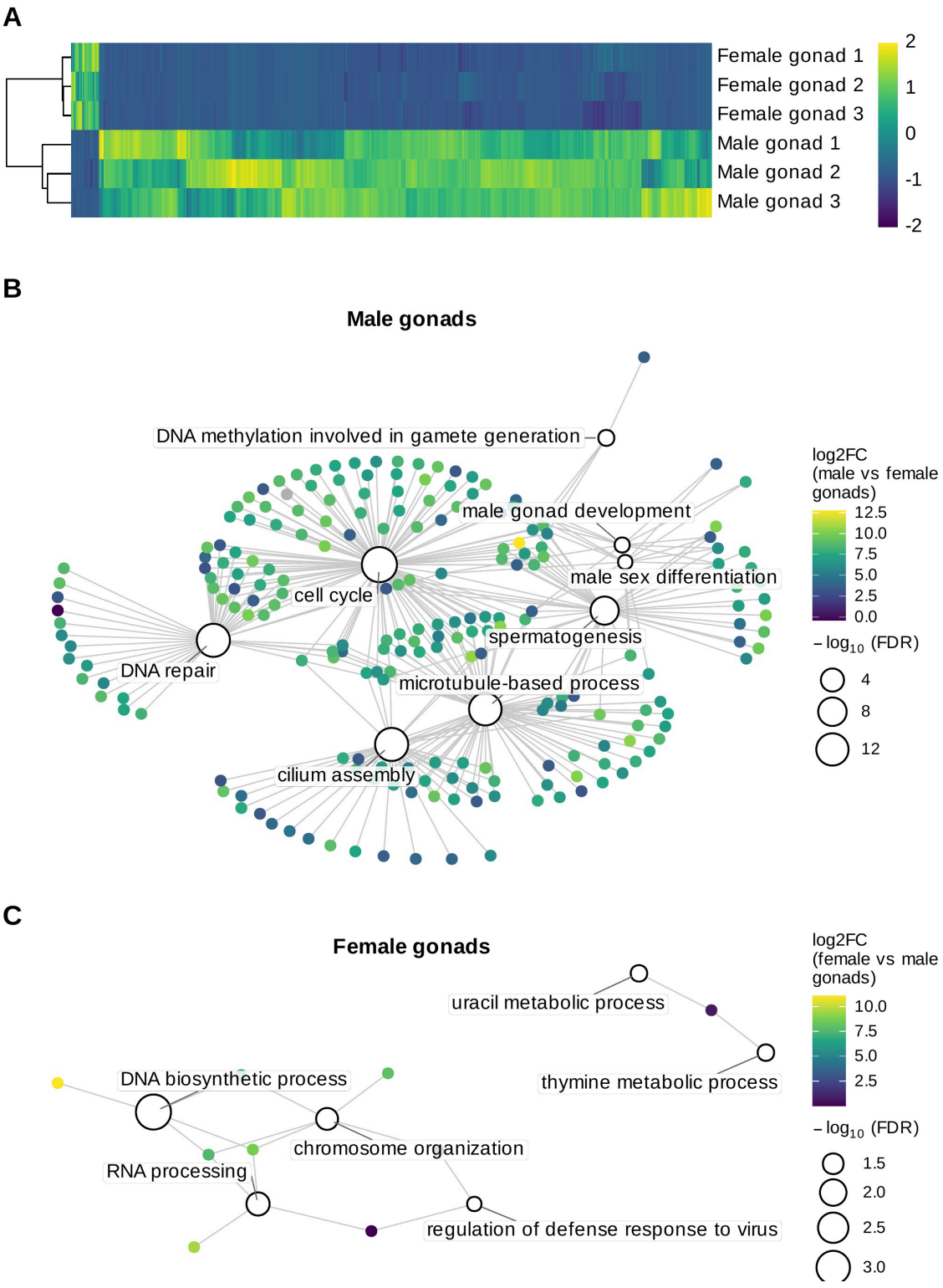

Figure 1

Gene expression patterns in gonads of the sexual species *Eiseniella andaluciana*. A: Heatmap of hierarchically clustered differentially expressed genes between male and female gonads. B: Gene networks showing enriched GO biological process terms among genes upregulated in male gonads. C: Gene networks showing enriched GO biological process terms among genes upregulated in female gonads.

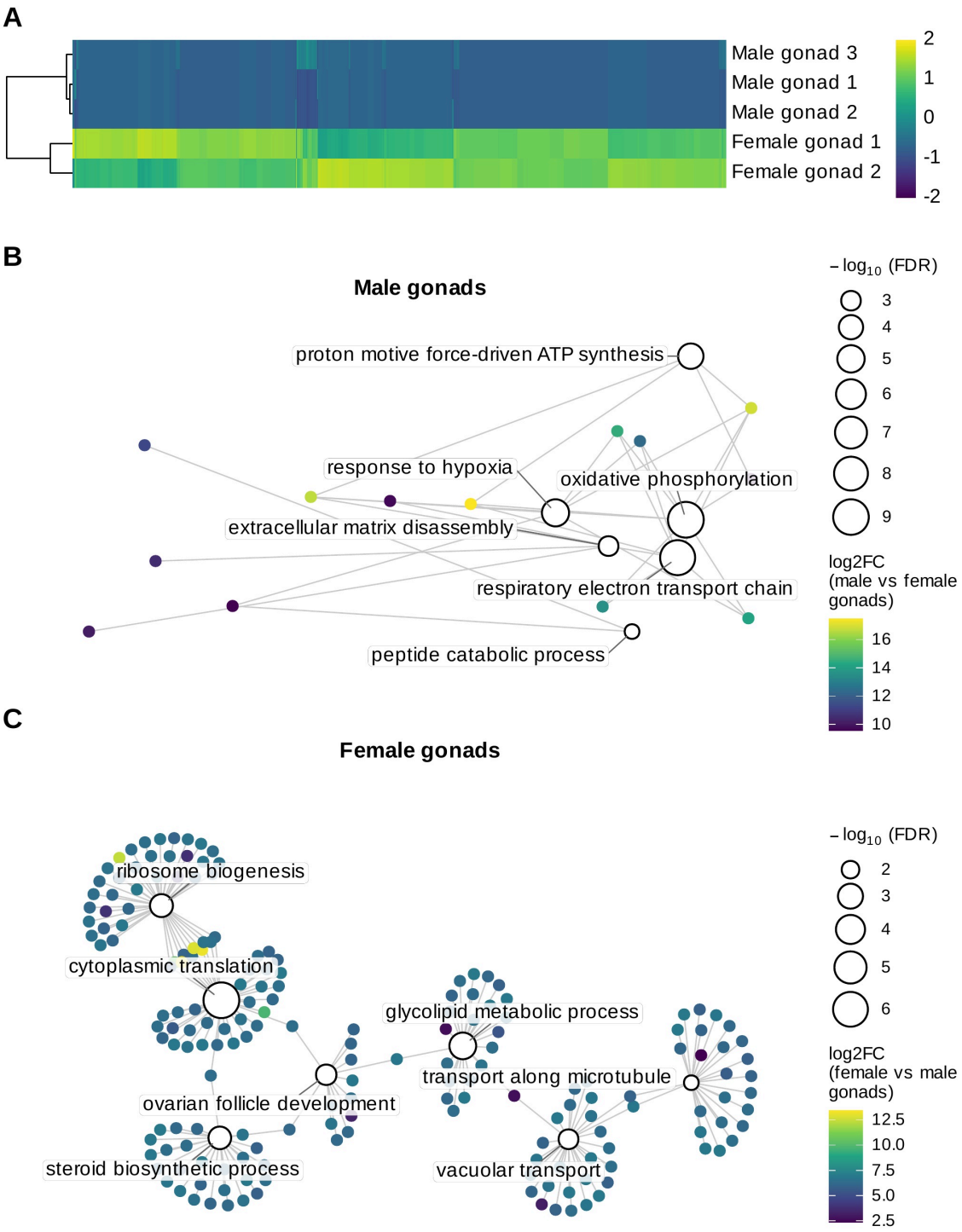

Figure 2

Gene expression patterns in gonads of the parthenogenetic species *Eiseniella tetraedra*. A: Heatmap of hierarchically clustered differentially expressed genes between male and female gonads. B: Gene networks showing enriched GO biological process terms among genes upregulated in male gonads. C: Gene networks showing enriched GO biological process terms among genes upregulated in female gonads.

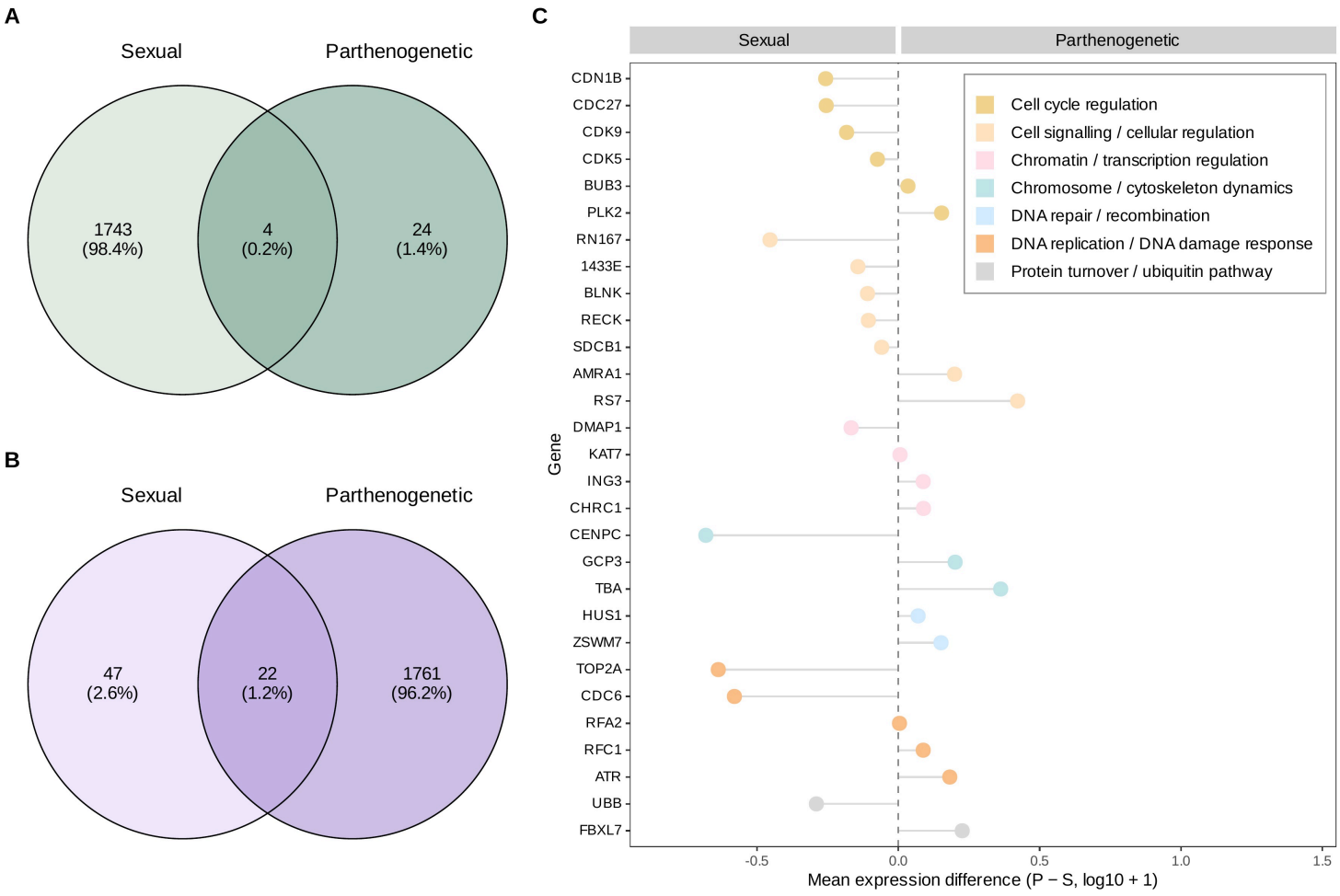

Figure 3

Comparison of gonadal gene expression between the sexual *E. andaluciana* and the parthenogenetic *E. tetraedra*. A: Venn diagram showing the number of genes upregulated in male gonads in each species and those shared between reproductive modes (FDR < 0.1 for *E. tetraedra*). B: Venn diagram showing the number of genes upregulated in female gonads in each species and those shared between reproductive modes. C: Lollipop plot showing the mean expression difference between parthenogenetic and sexual female gonads for selected orthologous genes associated with meiosis, cell cycle, DNA replication and DNA repair. Negative values indicate higher expression in sexual females and positive values higher expression in parthenogenetic females. Colours indicate the functional category of each gene.

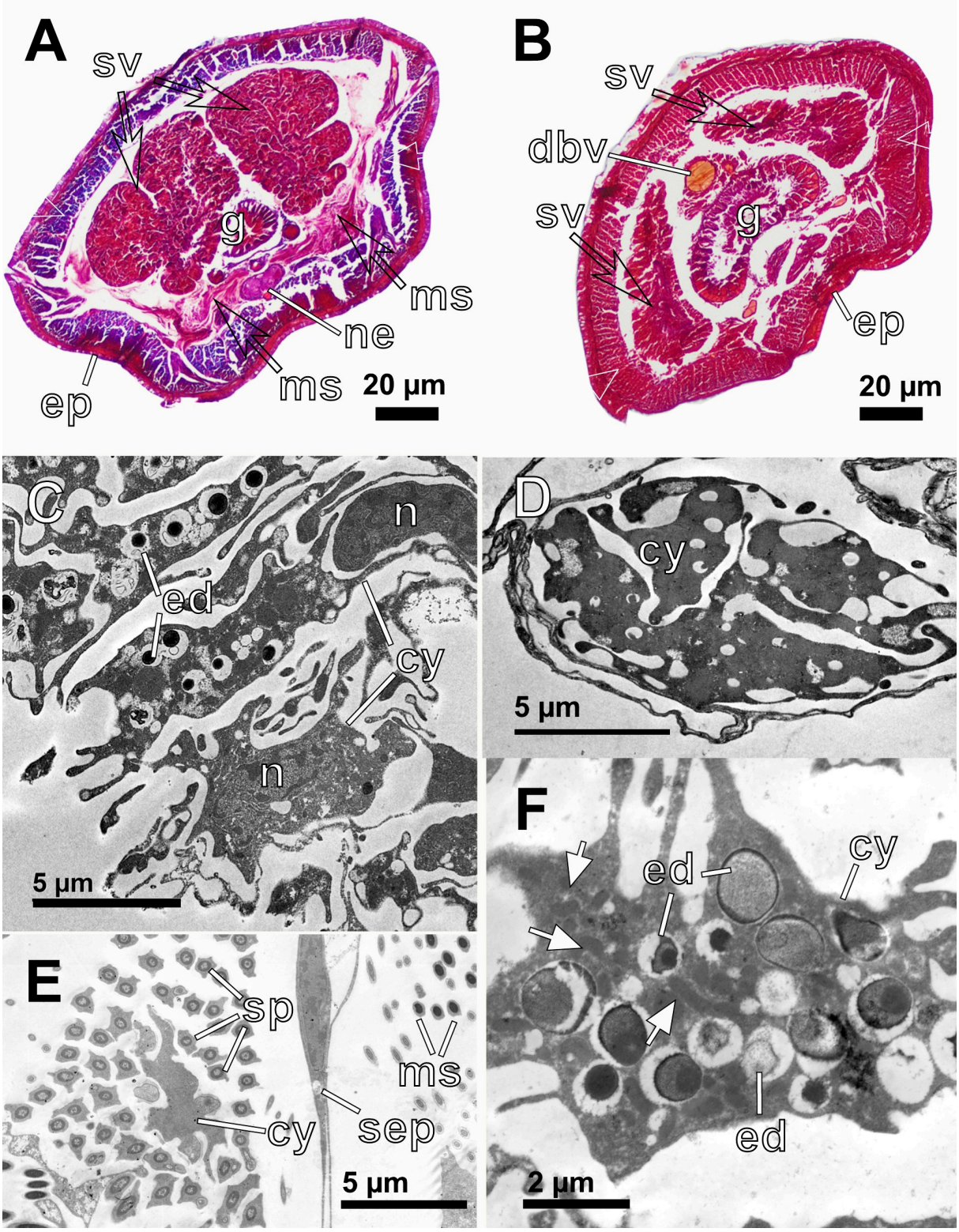

Figure 4

Light and transmission electron microscopy of the male reproductive region of both species. Left, sexual *E. andaluciana*; right, parthenogenetic *E. tetraedra*. A–B: Transverse sections through the male reproductive region (approximately segment 12) stained with Mallory's trichrome. A: *E. andaluciana*, showing large seminal vesicles (sv) densely packed with developing germ cells and abundant mature sperm (ms) in the male funnels. B: *E. tetraedra*, showing narrower seminal vesicles (sv) with fewer

developing germ cells and no mature sperm. Black arrows indicate the body wall musculature. C–D: Seminal vesicles of non-reproductive (juvenile) specimens. C: *E. andaluciana*, cytophores (cy) with nuclei (n) and electron-dense bodies (ed) in the cytoplasm. D: *E. tetraedra*, empty cytophore (cy) lacking associated germ cells. E–F: Seminal vesicles of reproductive (mature) specimens. E: *E. andaluciana*, cytophore (cy) surrounded by radiating spermatocytes (sp), with mature sperm (ms) in an adjacent compartment delimited by a separating cell (sep). F: *E. tetraedra*, empty cytophore (cy) producing electron-dense bodies (ed) resembling lipid or protein droplets; white arrows indicate mitochondria. Abbreviations: cy: cytophore; dbv: dorsal blood vessel; ed: electron-dense bodies; ep: epithelium; g: gut; ms: mature sperm; n: nucleus; ne: nerve axon; sep: separating cell; sp: spermatocytes; sv: seminal vesicle.

Supplementary Files

This is a list of supplementary files associated with this preprint. Click to download.

- SuppFig2PCAEtetraedra.pdf
- SuppFigurelegends.docx
- SupplementaryTableS1.xlsx
- SupplementaryFigure1.pdf
- SuppTablecaptions.docx
- SuppFig3heatmaporthologs.pdf
- SupplementaryTableS3.xlsx
- SupplementaryTableS2.xlsx
- Supplementaryfigure3.tif